European Journal of Cell Biology 90 (2011) 751–758

Contents lists available at ScienceDirect

European Journal of Cell Biology

journal homepage: www.elsevier.de/ejcb

Review

Lighting up the nuclear pore complex

Martin Kahms[a], Jana Hüve[a], Ramona Wesselmann[a], Julia C. Farr[a], Viola Baumgärtel[a], Reiner Peters[a,b,*]

[a] Institute of Medical Physics and Biophysics, and Center for Nanotechnology (CeNTech), University of Muenster, Heisenbergstrasse 11, 48149 Muenster, Germany
[b] The Rockefeller University, Laboratory of Mass Spectrometry and Gaseous Ion Chemistry, 1230 York Avenue, New York, NY 10065, USA

ARTICLE INFO

Keywords:
Nuclear pore complex
Nuclear transport
Transport model
Nuclear transport receptor
FG repeats
Super-resolution microscopy

ABSTRACT

It is generally accepted that transport through the nuclear pore complex (NPC) involves an abundance of phenylalanine–glycine rich protein domains (FG-domains) that serve as docking sites for soluble nuclear transport receptors (NTRs) and their cargo complexes. But the precise mechanism of translocation through the NPC allowing for high speed and selectivity is still vividly debated. To ultimately decipher the underlying gating mechanism it is indispensable to shed more light on the molecular arrangement of FG-domains and the distribution of NTR-binding sites within the central channel of the NPC. In this review we revisit current transport models, summarize recent results regarding translocation through the NPC obtained by super-resolution microscopy and finally discuss the status and potential of optical methods in the analysis of the NPC.

Introduction

The nuclear pore complex (NPC) is a large cellular structure spanning the nuclear envelope (NE). One of its major functions is mediating the transport of matter, energy and information between the cell nucleus and cytoplasm. In particular, the NPC selectively exports fully processed messenger ribonucleoprotein particles from the nucleus while retaining biosynthetic precursors. The NPC also selectively imports proteins into the nucleus that are necessary for the maintenance, replication, and transcription of the genetic material (for review see Peters, 2006; Wente and Rout, 2010). In addition, the NPC is involved in chromatin organization, gene activation and cell cycle regulation (for review see Strambio-De-Castillia et al., 2010; Wozniak et al., 2010). Thus, most basic functions of the cell, as well as many pathological conditions, are somehow related to the activity of the NPC. For this reason, the NPC has become a major object of biological, biochemical, and biophysical investigations. But though intensively studied, several questions regarding developmental and functional aspects of the NPC are poorly understood. How are single NPCs assembled *de novo* during interphase and integrated into the NE without loss of the permeability barrier? And *vice versa*, how are NPCs disassembled during mitosis? What is the role of the NPC in the regulation of gene expression and the internal architectural organization of the nucleus? And most intriguingly, what is the transport mechanism allowing for high speed and selectivity of cargo transport across the NE without direct involvement of motor proteins or enzymatic activity? In this article, we revisit the key features of nucleo-cytoplasmic transport and discuss current translocation models. We highlight recent progress in the analysis of structural and functional aspects of the NPC by super-resolution microscopy and finally discuss the status, prospect and implication of optical methods in the analysis of the NPC.

Structure of the NPC

The structure of single NPCs has been intensively studied using (cryo-) electron microscopy culminating in three dimensional (3D) models with 6–10 nm resolution (Beck et al., 2004, 2007; Stoffler et al., 1999). In addition, individual constituents have been crystallized and their structures solved at atomic resolution (Brohawn et al., 2009). According to these studies, the vertebrate NPC consists of an approximately cylindrical central scaffold measuring ~125 nm in diameter and ~70 nm in height containing a large channel of ~50 nm in diameter (Fig. 1). This central scaffold is composed of three connected rings, the cytoplasmic ring, the spoke ring and the nuclear ring, exhibiting on a gross level eightfold symmetry with regard to the central axis of the NPC, and twofold symmetry with regard to the plane of the NE. Eight filaments of ~50 nm

Abbreviations: NPC, nuclear pore complex; NE, nuclear envelope; Nup, nucleoporin; OSTR, optical single transporter recording; NTR, nuclear transport receptor; Kap, karyopherin; NLS, nuclear localization sequence; NES, nuclear export sequence; GEF, guanine nucleotide exchange factor; GAP, GTPase activating protein; ROD, reduction of dimensionality; PSF, point spread function; FWHM, full width at half maximum; GFP, green fluorescent protein; PALM, photoactivated-localization microscopy; SIM, structured illumination microscopy; STED, stimulated emission depletion.

* Corresponding author at: The Rockefeller University, Laboratory of Mass Spectrometry and Gaseous Ion Chemistry, 1230 York Avenue, New York, NY 10065, USA.
E-mail address: rpeters@mail.rockefeller.edu (R. Peters).

0171-9335/$ – see front matter © 2011 Elsevier GmbH. All rights reserved.
doi:10.1016/j.ejcb.2011.04.004

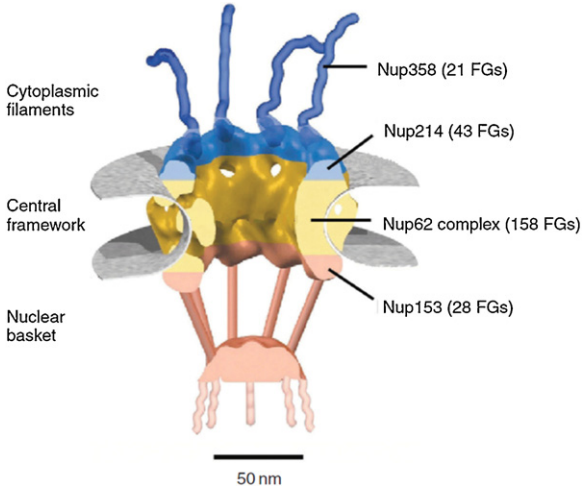

Fig. 1. Nuclear pore complex (NPC) architecture. The NPC essentially consists of a central scaffold (~125 nm in diameter and ~70 nm in height) spanning the nuclear envelope. Eight filaments are attached to the cytoplasmic face and extend into the cytoplasm. The nuclear face is also decorated with eight filaments which conjoin at their end to form a basket like structure. The localization of some nuclear pore proteins (Nups) is indicated together with the number of phenylalanine–glycine rich domains (FGs).
Adapted by permission from Macmillan Publishers Ltd.: Nature Reviews Molecular Cell Biology, copyright 2003 (Fahrenkrog and Aebi, 2003).

length are attached to the cytoplasmic ring. The nuclear ring is also decorated with eight filaments which distally conjoin to form a basket-like structure on the nuclear face. NPCs are composed of about 30 different proteins, known as nucleoporins or Nups (Cronshaw et al., 2002; Rout et al., 2000), that occur in multiples of 8, adding up to several hundreds of proteins per NPC. Nups contain only a few different folds and therefore the apparent complexity is reduced by a relatively simple modular architecture (Alber et al., 2007; Devos et al., 2006). Nups form three layers around the central axis of the NPC from which the most peripheral "membrane layer" contains cadherin folds and transmembrane helices anchoring the NPC within the NE. An intermediate "scaffold layer" is mainly composed of Nups with α-solenoids and β-propellers and finally, the most inner layer, composed of about one third of Nups, contains domains with multiple repeats of phenylalanine and glycine. Proteins of this inner layer are therefore termed FG-Nups. Interestingly, Nups seem to exhibit a certain level of redundancy and functional overlap in the NPC, as many Nups have been shown to be nonessential in yeast (Doye and Hurt, 1995).

Translocation through the NPC

Fluorescence microscopy has played a major role in studying functional aspects of the NPC. In combination with selectively permeabilized mammalian cells (Ribbeck et al., 1998; Ribbeck and Gorlich, 2001) and flux determination through single NPCs in isolated NEs of *Xenopus laevis* oocytes (optical single transporter recording, OSTR; Bradatsch et al., 2007; Keminer and Peters, 1999; Kiskin et al., 2003) fluorescence microscopy allowed for analysis of passive permeability, facilitated the diffusion of nuclear transport receptors (NTRs) and the participation of the small GTPase Ran in translocation cycles. Furthermore, nuclear transport has been analyzed by fluorescence microscopy in living cells by means of microinjection (Dange et al., 2008) and genetic manipulation (Timney et al., 2006). These studies revealed, that the NPC exhibits a contradictory functional duality as it allows selective transport of large cargo–NTR-complexes up to a size of ~40 nm in diameter (Pante and Kann, 2002), but at the same time prevents the passive diffusion of molecules larger then ~5 nm (Keminer and Peters, 1999). However, this high selectivity still comes along with high speed and parallelization of transport, as single NPCs can perform multiple translocation events per second, shuttling a mass of ~100 MDa or up to 1500 molecules per second and NPC (Ribbeck and Gorlich, 2001; Siebrasse and Peters, 2002). Specific and facilitated transport depends on cargo recognition by soluble NTRs that in turn interact with the NPC to carry their cargo across the NE (for review see Peters, 2006; Wente and Rout, 2010). The largest group of these NTRs is the highly conserved family of proteins known as karyopherins (Kaps). There are at least 20 members of the Kap-family (importins, exportins and transportins) in vertebrates (Pemberton and Paschal, 2005). Molecules carrying short signaling peptides, either a nuclear localization signal (NLS) or a nuclear export signal (NES), bind to their cognate Kap mostly directly. However, in some cases an accessory adapter protein is required. In addition to their cargo-binding domain, Kaps bear NPC-binding domains which directly interact with FG domains at the NPC (Bayliss et al., 2000; Chi and Adam, 1997). Cargo–receptor complexes are then transported through the NPC and released into the nucleus in import cycles or into the cytoplasm in export cycles. The docking and translocation of Kap–cargo complexes is not directly energy dependent but directionality is driven by a gradient of the small GTPase Ran that exists in two different configurations, either bound to nucleotide guanine triphosphate (RanGTP) or guanine diphosphate (RanGDP) (Izaurralde et al., 1997). This gradient is established by a set of proteins, distinctly localized in the cytoplasm and nucleoplasm. The Ran guanidine exchange factor (RanGEF, RCC1 in vertebrates) which promotes the exchange of guanine nucleotides, is bound to chromatin and therefore is exclusively found in the nucleus where it generates a high nuclear concentration of RanGTP (Bischoff and Ponstingl, 1991). RanGTPase activating protein (RanGAP) localizes to the cytoplasm or attaches to the nuclear face of the NPC and catalyzes rapid conversion of cytoplasmic RanGTP to its GDP-bound form (Mahajan et al., 1997). This unequal distribution of RanGTP is the basis for directionality of transport through the NPC. For import, Kaps recognize their cognate cargo in the cytoplasm where the RanGTP concentration is low. Once the complex has moved through the NPC, release and complex dissociation are stimulated by high nuclear levels of RanGTP. In return, exporting Kaps can bind to their cargo only in the presence of RanGTP in the nucleus and on translocation and arrival at the cytoplasmic side of the NPC, the export complex is dissociated by hydrolysis of RanGTP (Lee et al., 2005).

Transport models

Although the structure and function of the NPC have been intensively studied over the last years, the mechanism of selective gating still remains unclear. Several models of translocation have been proposed, trying to explain the remarkable features of the NPC in terms of translocation speed and selectivity on a molecular level. As a common feature, all these models imply that the gross structure of the NPC is maintained and instead, transport is based on local stochastic molecular interactions within the NPC. In this sense, all current models of transport through the NPC can be brought into one common framework, namely virtual gating. The expression "virtual gating" was first introduced by Rout et al., to characterize the nature of a specific transport model, Brownian affinity gating (Rout et al., 2003). But in a more generalized perception, virtual gating is an inherent feature of most of the representative transport models. This section briefly summarizes some of the proposed transport mechanisms.

Brownian affinity model

The Brownian affinity model (Rout et al., 2003) assumes that filamentous FG-Nups prevent non-binding molecules from entering the central channel by rigorous thermal motion. Molecules have to pay an entropic price to move through the pore that increases with their size and thereby lowers their probability of crossing the channel. Interaction of transport receptors with FG-Nups increases the probability of entering the channel and thus facilitates the translocation step as long as binding is not too strong and is rapidly reversible. The translocation itself occurs by Brownian motion.

Affinity gradient model

According to the affinity gradient model, NTR–cargo complexes bind to FG repeats which are positioned to have progressively increasing affinity for the NTR along the central channel. This affinity gradient is thought to promote migration towards the other end of the NPC. Evidence for such a gradient came originally from quantitative analysis of the interaction between mammalian Kapβ1 and a set of distinct Nups, which are asymmetrically distributed within the NPC (Ben-Efraim and Gerace, 2001). Later, similar findings were reported for the yeast NTR Kap95p (Pyhtila and Rexach, 2003).

Selective phase model

The selective phase model (Ribbeck and Gorlich, 2002) assumes that FG repeat domains of Nups are connected by weak hydrophobic interactions and form a sieve-like meshwork occupying the lumen of the central channel. This network is supposed to have the properties of a hydrogel and to prevent the passage of inert molecules that are larger than its pore size. Transport receptors are thought to move through by locally dissolving or "melting" the FG–FG interactions. In this context, it was shown that concentrated solutions of recombinant FG-domains can form a hydrogel *in vitro* (Frey et al., 2006) and display properties in terms of molecular uptake that are partially reminiscent of the transport characteristics of the NPC (Frey and Gorlich, 2007).

Reduction of dimensionality (ROD)

Because of the high density of FG repeats with a mean distance of 3–6 nm, the ROD model predicts that the FG domains yield one coherent hydrophobic layer coating the wall of the transport channel and the surface of the filaments (Peters, 2005). Passive diffusion is restricted by a loose network of peptide chains that only spare a narrow central channel of 8–10 nm in diameter. Binding transport complexes is brought about by multiple hydrophobic interactions between FG motifs and binding spots on the NTRs, yielding a firm attachment of NTRs and transport complexes to the FG layer but, at the same time, granting a high mobility in the plane of the FG layer. This scenario opens the possibility that bound transport receptors move along the walls of the central channel in a two-dimensional random walk instead of three dimensional Brownian motion. When encountering a channel exit, the transport complexes are exposed either to a high concentration of RanGTP (on the nuclear side) or RanGAP (on the cytoplasmic side), which causes their release from the FG layer and their disassembly.

Reversible FG domain collapse

As indicated by atomic force microscopy data, the peptide chains of FG-repeats exhibit a polymer-brush-like configuration when tethered to a surface (Lim et al., 2006). By this means, they are thought to form a large corona around the entrances of the NPC which rejects non-binding molecules via entropic exclusion. In the presence of an interacting NTR, the FG domains collapse and draw the transport complex into the transport channel (Lim et al., 2007). In the transport channel, the transport complex undergoes cycles of binding and unbinding until it reaches the transport channel exit. Finally, interaction with RanGTP leads to complex release and the FG-repeats return to their original conformation.

Forest model

Recently, it was reported that FG-domains can be classified into two main categories (Yamada et al., 2010). FG domains with low charge content adopt a globular collapsed coil conformation while others are highly charged and prefer a dynamic, extended coil conformation. The distribution of these two types of FG-domains within single Nups featured a non-random, bimodal distribution. For this reason, the authors suggested a topology of FG-domains in the central channel, in which FG domains with sticky globular conformations are located at the tip of FG-Nups and conjoin to define the properties of the most inner region of the central channel (central zone). These globular FG-Nups are connected to the NPC scaffold via FG domains in a relaxed or extended conformation (stalk zone). This proposed arrangement features two separate zones of traffic with distinct physicochemical properties. The stalk zone allows for translocation of NTRs alone or NTRs loaded with small cargos. In this region transport is mediated by interaction of NTRs with the extended coil FG-domains keeping the NTRs suspended in the conduit and adding fluidity to the area. In contrast, Kaps carrying large cargos, e.g. large mRNPs and ribosomes, have to pass through the central zone because the diameter of the spared region in the central zone can be expanded. This expansion might be a direct consequence of NTR binding in the stalk zone, leading to a collapse of the extended coil FG-domains and therefore retraction of the globular FG-domains.

Interaction between FG-Nups and NTRs

It is generally accepted that translocation through the NPC involves a large channel and an abundance of FG domains which serve as interaction sites for NTRs and their cargo complexes. To further elucidate the mechanism of transport on a molecular level it is essential to shed more light on the arrangement of FG domains and their interaction with NTRs. About one-third of Nups contain so-called FG domains. Each of these domains consists of up to 50 FG repeats, yielding together ~190 FG domains with a total of ~2700 FG motifs per NPC (Peters, 2009). FG repeats consist of hydrophobic amino acid motifs such as FG, FXFG, or GLFG and hydrophilic linkers of 5–50 amino acid residues. These domains display similarities to natively unfolded or intrinsically unstructured proteins which are highly flexible and lack secondary structure in their native state (Denning et al., 2003). In general, intrinsically disordered protein domains, which are very common in eukaryotic proteins, undergo structural transitions to folded forms upon binding of ligands (Fink, 2005). FG motifs serve as binding sites for NTRs and early studies suggested a number of two or three distinct FG interaction sites on NTRs like Kapβ1 and NTF2 (Bayliss et al., 1999; Chi and Adam, 1997). Molecular dynamics simulations, however, revealed that NTRs may contain up to seven additional FG-binding sites (Isgro and Schulten, 2005, 2007), implying that the surface of NTRs displays a virtually coherent FG-binding stripe, instead of a few distinct binding sites. The binding affinities of NTRs to FG domains have been quantitated in several studies. It has been reported, that the binding strength of FG domains derived from several vertebrate Nups for the NTR Kapβ1 is rather high with apparent k_D values ranging from 10 to 200 nM (Ben-Efraim and Gerace, 2001). Based on these affinities and the assumed localization of the particular FG domains

within the NPC transport channel, the affinity gradient model was proposed involving an affinity gradient that steeply increases from the cytoplasmic to the nuclear side of the NPC transport channel. The binding strength of NTRs for FG domains can be modulated by other ligands. Thus, binding of an NLS protein to the NTR usually increases its binding strength for FG motifs, while binding of RanGTP to importing NTRs, even at low RanGTP concentrations, virtually abolishes binding. Recently, the binding of NTRs to NPCs has been quantitated by fluorescence correlation spectroscopy (FCS) and single-molecule fluorescence microscopy. In living neuroblastoma cells, NPCs or their immediate environments were found to bind 104 Kapβ, 48 Kapα, 43 Ran, and 6 NTF2 molecules per NPC (Paradise et al., 2007). In mammalian permeabilized cells, individual NPCs were found to display two types of binding sites for Kapβ1, one characterized by an effective k_D value of 0.3 nM and a maximum of 7 molecules bound per NPC, and the other by an effective k_D value of 70 nM and a maximum of 110 molecules bound per NPC (Tokunaga et al., 2008). But the latter values might represent a lower limit for binding capacity because of endogenous NTRs which could not be removed completely in this kind of preparation. And indeed, results obtained on isolated nuclei of yeast suggest an even higher binding capacity for NTRs in single NPCs (Farr, 2009). But as both, NTRs and FG domains have multiple binding sites the reported k_D values are not dissociation constants of single pairs of FG motifs and NTR binding sites but the effective dissociation constants of the overall association reaction. Since in such cases the binding strength, also referred to as avidity, is the product, not sum, of the individual dissociation constants, the single-pair dissociation constants may be indeed rather large. But in general, these results indicate strong binding of NTRs to the NPC and high capacity of binding sites at single NPCs. As the cytoplasmic concentrations of NTRs, like mammalian Kapβ1 and yeast Kap95p, have been found to be in the micromolar range (Paradise et al., 2007; Pyhtila and Rexach, 2003), i.e. orders of magnitude above the effective k_D values of FG–NTR complexes (Ben-Efraim and Gerace, 2001; Pyhtila and Rexach, 2003), it is likely that under physiological conditions the NPC is saturated with NTRs. In such an arrangement NTRs cannot be regarded as soluble interaction partners but instead, constituent parts of the NPC. Indeed, this assumption is supported by the fact that a simple device – an artificial nanotube coated with FG Nups – displayed many of the features of nuclear transport (Jovanovic-Talisman et al., 2009). The flux of fluorescently labeled compounds through the nanotubes was analyzed revealing that NTRs and their cargo complexes were transported much faster than molecules of similar size that do not bind to FG domains. Selectivity was solely dependent on the diameter of the nanopores, the length of the FG domain-coated part of the nanopores and the binding strength of the FG–Kap pairs. Importantly, the NPC-like transport specificity depended on the presence of NTRs. In the absence of NTRs, non-binding molecules passed through the nanopores as fast as NTRs of comparable size at rates expected from a hydrodynamic theory.

Lighting up the NPC by super resolution microscopy

A deeper understanding of the NPC requires detailed information on both its molecular structure and function. Classically, the structure of the NPC has been analyzed by electron microscopy. But the NPC has to be regarded as a highly dynamic structure (Rabut et al., 2004) and several components of the nuclear pore complex exhibit a rather low affinity and are easily lost during classical preparation procedures. In addition, recent results suggest that transport factors cannot be regarded as transient interaction partners mainly present in the soluble phase, but instead are indispensable components of the selectivity barrier. Therefore it is virtually impossible to study the intact nuclear pore outside the living cell. Among the currently available methods for the analysis of protein complexes in living cells, fluorescence microscopy appears to be the most promising candidate as it allows for live cell imaging, molecular specificity, high time resolution and spectral multiplexing, and at the same time can be regarded as minimally invasive. However, an obvious shortcoming of conventional fluorescence microscopy is spatial resolution. But recent progress in the applicability of concepts, that overcome the classical resolution limit in light microscopy, has opened a highly attractive perspective to analyze single protein complexes in living cells and tissues. The distribution of NPCs in the NE was first visualized by light microscopy on fixed mammalian cells stained with an antibody against an NPC component (Kubitscheck et al., 1996). The resulting punctuate pattern was analyzed by a combination of confocal microscopy and image analysis. Although the structure of single NPCs could not be resolved, their area density (10 NPCs per μm^2) allowed for imaging single NPCs as diffraction-limited spots. Several years later, scanning near-field optical microscopy was employed to study the distribution of NPCs in isolated NEs of *Xenopus laevis* oocytes (Hoppener et al., 2005). A lateral resolution of ~50 nm was achieved and single NPCs were resolved by scanning either the nuclear or cytoplasmic surface of the NE under near-physiological conditions. As the NE of *Xenopus laevis* oocytes display a much higher density of NPCs, with a mutual distance of 120 nm, it is virtually impossible to resolve single NPCs in these preparations by means of classical light microscopy. But besides this near-field approach, featuring a variety of intrinsic limitations, much progress has been made in the last decade to overcome the classical resolution limit using wide-field microscopy allowing for functional and structural analyses of the NPC with nanometer resolution in unfixed cellular preparations and living cells.

Single molecule fluorescence microscopy

Single molecule microscopy has proven to be a powerful tool in the analysis of single translocation events, as well as structural features of single NPCs, with nanometer precision. Using a highly sensitive microscope setup, single molecules can be resolved as diffraction limited spots. The precision by which the center of these spots can be localized depends on the FWHM of the PSF, the number of collected photons, the background intensity, and the pixel size of the detector (Thompson et al., 2002). Experimentally, localization precisions of ~1.5 nm (500-ms sampling time) and ~10 nm (400 μs sampling time) have been achieved (Ma and Yang, 2010; Yildiz et al., 2003). Employing single molecule fluorescence microscopy the translocation of single NTRs and transport complexes through the NPC has been intensively analyzed. Binding of NTF2, a Ran specific NTR was studied in permeabilized HeLa cells constitutively expressing the GFP-tagged Nup POM121 (Kubitscheck et al., 2005). The dwell time distribution of single fluorescently labeled NTF2 at the NPC could be fitted by a single-exponential function with a time constant of 5.8 ± 0.2 ms, which was slightly decreased when NTF2 was loaded with its cognate substrate. Similar dwell times have been reported for a fluorescently labeled substrate (NLS-2xGFP) in the presence of its cognate NTR in permeabilized cells (Yang et al., 2004). This kind of analysis has been recently extended to living cells and upon microinjection of nanomolar concentrations of labeled NTRs (Kapβ1, Kapβ2, Kapα2) and a model substrate (BSA-NLS), the histograms of binding durations revealed dwell times at the NPC ranging from 4 to 10 ms (Dange et al., 2008), values in good agreement with estimates in the permeabilized preparations mentioned above. On a first view, these dwell times appear surprisingly low, as a single NPC is capable of transporting up to 1500 molecules per second (Siebrasse and Peters, 2002), but sequential translocation of substrates with a dwell time from 5 to 10 ms would

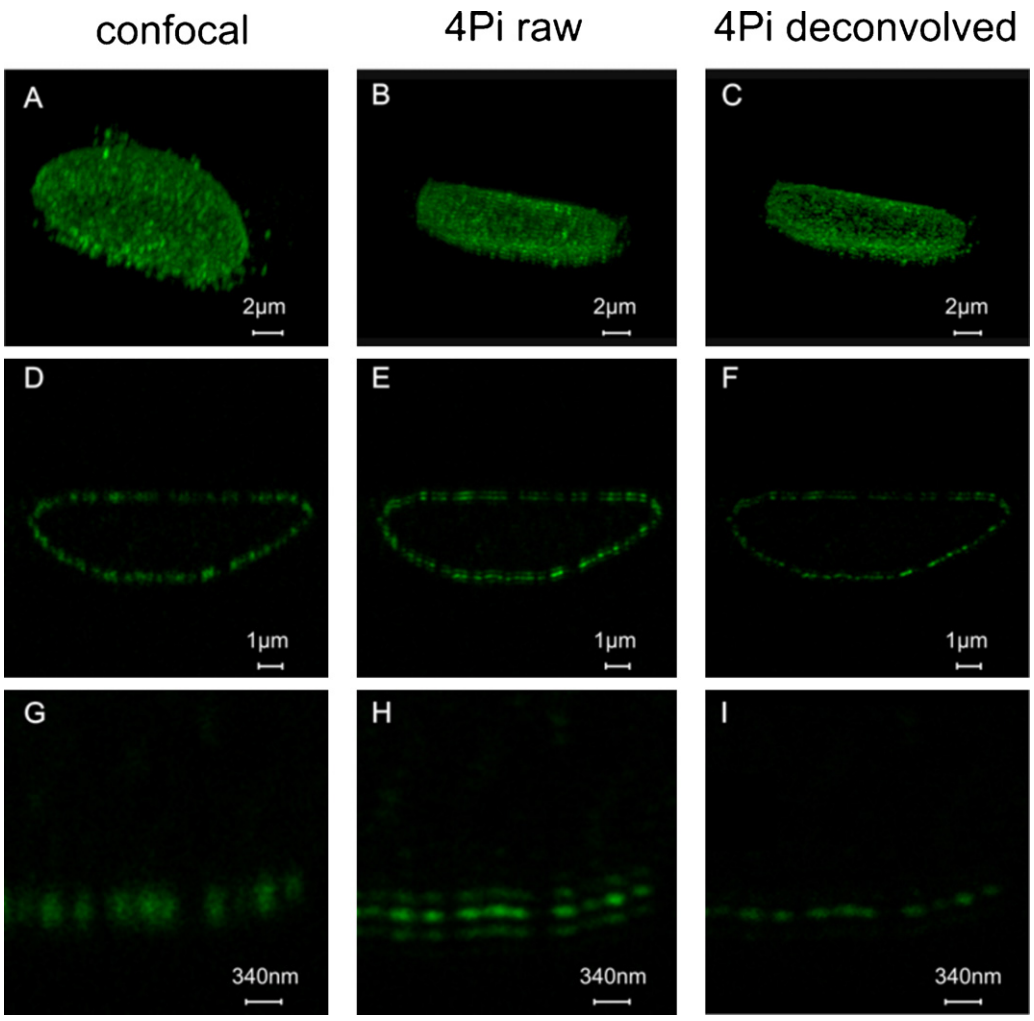

Fig. 2. 4Pi imaging of single NPCs. HeLa cells were labeled by immunofluorescence using a primary antibody against the NPC protein Nup358 and an Alexa 488-labeled secondary antibody. (A–C) 3D reconstruction of the distribution of NPCs in the nuclear envelope, derived from a series of axial optical sections by confocal (A) and 4Pi (B) microscopy. The effect of side lobe removal by deconvolution is shown in C. (D–F) Single axial sections of a HeLa cell nucleus. (G–I) A detailed view of single NPCs showing the increase in axial resolution obtained with 4Pi microscopy.
Taken from Hüve et al. (2008).

only allow for a maximal transport rate of 100–200 molecules per second per NPC. Therefore it is the most likely scenario that the NPC is capable of performing several translocations at the same time which is in principle compatible with most of the translocation models discussed above. In addition, single molecule studies have provided valuable insights into the spatial distribution of single Nups and interaction sites at the NPC. Single binding events of an antibody directed against Nup358 could be localized in dual color experiments with a maximum at a distance of 70 nm towards the cytoplasmic face of the NPC relative to the center defined by the localization of POM121-GFP, a transmembrane protein anchoring the NPC in the NE (Kubitscheck et al., 2005). This result was in perfect agreement with electron microscopy studies. Furthermore, binding sites of NTF2 at the NPC were analyzed in relation to POM121-GFP. The results showed that binding occurred all along the NPC axis, with a maximum slightly displaced to the cytoplasmic side of the NPC center, but not at the periphery of the NPC. Similar results were obtained upon microinjection of fluorescently labeled molecules (Kapβ1, Kapβ2, Kapα2 and BSA-NLS) into living cells (Dange et al., 2008). Binding of NTRs and cargo complexes was observed only in the central region of the NPC and occurred neither predominantly at the cytoplasmic nor at the nucleoplasmic filaments. For this reason, single molecule studies gave no indication of a putative affinity gradient along the NPC or a large cloud of NTR binding sites surrounding the cytoplasmic entrance. These observations were further substantiated by single molecule experiments, in which bound cargo molecules were tracked during their dwell time (Yang et al., 2004). The reported trajectories suggest that molecules perform a random walk in the central channel of the NPC before they exit either at the nucleo- or cytoplasmic face. Therefore the NPC itself does not provide directionality and the release site of bound molecules is determined by additional factors. Recently, a three dimensional density map of transient interactions at the NPC has been constructed based on single molecule experiments employing inclined illumination with a spatiotemporal resolution of 9 nm and 400 μs (Ma and Yang, 2010). The authors observed a gradual increase of interaction density from both sides of the NPC towards the center of the NPC for both cargo-free and cargo-loaded Kapβ1. The density was highest in the central pore region but a central axial channel of 10–20 nm was seldom occupied. Non-FG-interacting molecules instead are gradually barricaded on the cytoplasmic face and are further inhibited in the central pore region. The authors concluded that the pathway for facilitated translocation depends more on the localization of interaction sites for NTRs than on general NPC architecture. In addition to protein transport, translocations of single endogenous β-actin RNA

molecules labeled by yellow fluorescent protein were analyzed by dual color single molecule fluorescence microscopy (Grunwald and Singer, 2010). The reported data claim that major interaction sites of mRNA complexes are located at the NPC surface rather than within the central channel. This result might indicate that mechanistically the export of RNA differs substantially from translocation of protein cargos.

4Pi microscopy

In 4Pi microscopy, a laser beam is split into two beams and directed through two opposing objective lenses onto the object (Hell and Stelzer, 1992). The wave fronts of the illuminating beams are adjusted to constructively interfere in a common focus. This yields an interference pattern, which essentially consists of a main focal spot and two smaller side lobes. At optimal conditions, the main peak of the PSF has a FWHM of 100 nm in the direction of the optical axis, and thus is 6–7-fold smaller than that of a confocal PSF (Fig. 2). The localization precision of diffraction limited signals scales with $\sim \mathrm{FWHM}/\sqrt{n}$ with n being the number of photons detected (Thompson et al., 2002), meaning that improved optical resolution, at least in principle, provides higher accuracy. Therefore 4Pi microscopy has been applied to fixed immune labeled cells to unravel the topography of the NPC by means of 4Pi microscopy (Hüve et al., 2008). With an axial resolution of 110–130 nm and a dual color colocalization accuracy of 5–10 nm, the distance between epitopes located at the tip of the cytoplasmic filaments and at the ring of the nuclear basket could be clearly resolved with an estimated distance of ~150 nm. In cells expressing a green fluorescent protein construct localized at the NPC center (POM121), the distances between the ring of the nuclear filaments and the NPC center and the distance between the NPC center and the tip of the cytoplasmic filaments were determined to be ~90 and ~85 nm respectively (Fig. 3). All these values were in good agreement with previous electron or single-molecule fluorescence estimates. The latter study was performed on fixed specimens using glycerol immersion lenses but this kind of analysis was subsequently extended to physiological conditions employing water immersion lenses. This configuration allowed for studying binding of NTRs and transport complexes in intact NPCs in permeabilized cells by means of 4Pi microscopy (Kahms et al., 2009). It was found that the direct binding sites of the GTPase Ran had a maximum at approximately 30 nm towards the cytoplasm with regard to the NPC center, whereas in the presence of its cognate NTR NTF2, a redistribution of Ran could be observed with binding sites shifted by approximately 20 nm towards the NPC center. This shift could be only clearly resolved by 4Pi microscopy because of a two to threefold improved localization precision as compared with single-molecule microscopy. Binding site distributions of the NTR Kapβ1 and a Kapβ1-based transport complex also revealed maxima slightly displaced to the cytoplasmic side of the NPC by approximately 10 nm. In accordance with single molecule studies, these observations support transport models in which NTR binding sites are distributed all along the transport channel.

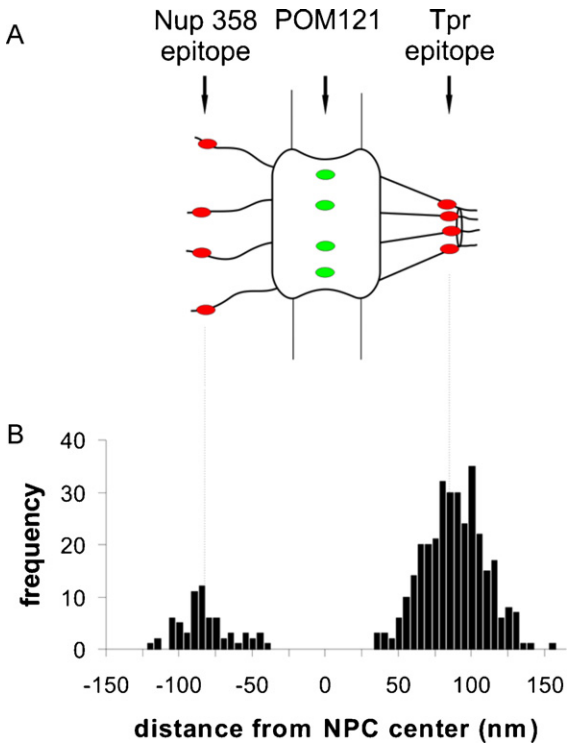

Fig. 3. Distance between molecular sites in single NPCs as determined by two-color localization 4Pi microscopy. (A) Sketch of the NPC indicating the positions of the sites that were fluorescently labeled: an epitope on Nup358 at the tips of the cytoplasmic filaments, a site at the center of the NPC (GFP construct of POM121), and an epitope on Tpr localized at the ring of the nuclear basket. (B) Distances measured in single NPCs of NRK cells between the Tpr epitope and Pom121-GFP and between Pom121-GFP and the Nup358 epitope.
Adapted from Hüve et al. (2008).

Conclusions and perspectives

Transport through the NPC involves translocation of a multitude of substrates. Remarkably, translocation seems to be massively parallel, bidirectional, selective and fast. Paradoxically, the speed of the translocation process is enhanced for molecules which are able to interact with the NPC compared to non-interacting molecules. Obviously, no motor proteins or NTPases are directly involved in the translocation process and furthermore, no conformational changes have been reported in conjunction with the translocation process. To account for this mystery, several models have been proposed, trying to translate the macroscopic features of the NPC into nanoscopic molecular organization. But recent results make it necessary to reconsider the translocation mechanism. First, NTRs have a high affinity towards FG-domains of the NPC. In combination with a high abundance of NTRs in a single cell and a high abundance of FG-domains within the NPC, they should be considered as genuine constituents of the NPC, saturating the NPC under physiological conditions. Second, super-resolution microscopy revealed binding sites for NTRs throughout the central framework with a lack of prominent binding sites at the periphery of the NPC. Third, cargos appear to move randomly within the central channel before they enter either side of the NPC, without directionality provided by the NPC itself. Fourth, data on nanopores with NPC-like transport selectivity suggest, that rejection of non-binding molecules was not brought about by the FG coat alone but required both FG coat and NTRs. Taken together, these data suggest, that the FG-domains coating the wall of the transport channel and eventually parts of the surface of the filaments, are saturated with NTRs. In this scenario, as originally proposed in the ROD model (Peters, 2005), the FG domains provide a semi-fluid, adaptable layer coating the channel wall and the surface of the filaments and thus fill in any roughness of the NPC scaffold, providing a smooth interface for adhering NTRs. NTRs bound to the channel wall define the permeability barrier and, unlike proposed in several transport models, the FG domains do not participate directly in the rejection of non-FG-binding molecules (Peters, 2009). This model is further supported by the finding that the interaction density of NTRs gradually increases from both sides towards the NPC center but spares an axial channel of ~20 nm, excluding the

existence of a single entropic barrier or the formation of a hydrogel meshwork. But to confirm this hypothesis it is indispensable to further elucidate the nanoscopic arrangement of FG domains and the distribution of NTRs in the central channel of the NPC in living cells. Fluorescence microscopy, classically limited in resolution to ~200 nm, has recently approached the nanometer domain providing the analytical power to light up the NPC with nanometer precision. Single molecule analyses, though still diffraction limited, yielded valuable insights concerning translocation of single transport complexes through the NPC with 9–30 nm precision at 0.4–5 ms time resolution. But there is still room to enhance both localization precision and time resolution, by improved instrumentation, brighter probes (Lowe et al., 2010) or a sophisticated alignment procedure in dual color experiments (Grunwald and Singer, 2010). In combination with photoswitchable fluorophores (PALM, photoactivated-localization microscopy; Betzig et al., 2006; Hess et al., 2009) and tracking techniques for three dimensions (Mlodzianoski et al., 2009), single molecule techniques have a high potential to further decipher the mechanism of nucleo-cytoplasmic transport. In contrast, a true increase in resolution is provided by 4Pi microscopy and structured illumination microscopy (SIM) and both techniques have been employed to unravel the topography of single NPCs (Hüve et al., 2008; Schermelleh et al., 2008). However, in 4Pi microscopy and SIM, gain in resolution is limited to ~100 nm and therefore both techniques, at least in their current implementation, lack the analytical power to shed light on the molecular arrangement within the central channel of the NPC. It has been reported, that SIM in combination with nonlinearity provided by excited state saturation of fluorophores theoretically provides unlimited resolution (Gustafsson, 2005). But the applicability of this technique in living cells has yet to be tested. One of the most promising candidates for the optical analysis of single protein complexes like the NPC is stimulated emission depletion (STED) microscopy. In STED microscopy, a diffraction limited laser beam is employed to excite fluorescence in a spot of the specimen. A red-shifted doughnut shaped "STED beam" is used to quench the fluorophores during the few nanoseconds they remain in their excited state by means of stimulated emission. The size of the doughnut and the relative position are adjusted such that the edges of the spot excited by the first laser pulse are depleted. As the optically induced transition to the ground state is saturable, the excitation spot can be trimmed down to dimensions, solely depending on the intensity of the "STED beam" providing theoretically unlimited resolution. Using STED-microscopy on fixed specimens a true optical resolution down to ~20 nm in a single optical plane (Donnert et al., 2006) or, employing a different optical configuration, an isotropic resolution of ~40 nm (Schmidt et al., 2008) has been reported, and even in living cells, a resolution of <50 nm is feasible (Hein et al., 2008). In combination with two-color STED (Schmidt et al., 2008), this methodology can be regarded as a valuable tool to study the arrangement of FG domains and binding site distribution of NTRs in the central channel of the NPC, lightning further up the molecular basis for this intriguing gating mechanism.

Acknowledgement

This work was supported by the Deutsche Forschungsgemeinschaft (SFB431, project P21).

References

Alber, F., Dokudovskaya, S., Veenhoff, L.M., Zhang, W., Kipper, J., Devos, D., Suprapto, A., Karni-Schmidt, O., Williams, R., Chait, B.T., Sali, A., Rout, M.P., 2007. The molecular architecture of the nuclear pore complex. Nature 450, 695–701.

Bayliss, R., Littlewood, T., Stewart, M., 2000. Structural basis for the interaction between FxFG nucleoporin repeats and importin-beta in nuclear trafficking. Cell 102, 99–108.

Bayliss, R., Ribbeck, K., Akin, D., Kent, H.M., Feldherr, C.M., Gorlich, D., Stewart, M., 1999. Interaction between NTF2 and xFxFG-containing nucleoporins is required to mediate nuclear import of RanGDP. J. Mol. Biol. 293, 579–593.

Beck, M., Forster, F., Ecke, M., Plitzko, J.M., Melchior, F., Gerisch, G., Baumeister, W., Medalia, O., 2004. Nuclear pore complex structure and dynamics revealed by cryoelectron tomography. Science 306, 1387–1390.

Beck, M., Lucic, V., Forster, F., Baumeister, W., Medalia, O., 2007. Snapshots of nuclear pore complexes in action captured by cryo-electron tomography. Nature 449, 611–615.

Ben-Efraim, I., Gerace, L., 2001. Gradient of increasing affinity of importin beta for nucleoporins along the pathway of nuclear import. J. Cell Biol. 152, 411–417.

Betzig, E., Patterson, G.H., Sougrat, R., Lindwasser, O.W., Olenych, S., Bonifacino, J.S., Davidson, M.W., Lippincott-Schwartz, J., Hess, H.F., 2006. Imaging intracellular fluorescent proteins at nanometer resolution. Science 313, 1642–1645.

Bischoff, F.R., Ponstingl, H., 1991. Catalysis of guanine nucleotide exchange on Ran by the mitotic regulator RCC1. Nature 354, 80–82.

Bradatsch, B., Katahira, J., Kowalinski, E., Bange, G., Yao, W., Sekimoto, T., Baumgartel, V., Boese, G., Bassler, J., Wild, K., Peters, R., Yoneda, Y., Sinning, I., Hurt, E., 2007. Arx1 functions as an unorthodox nuclear export receptor for the 60S preribosomal subunit. Mol. Cell 27, 767–779.

Brohawn, S.G., Partridge, J.R., Whittle, J.R., Schwartz, T.U., 2009. The nuclear pore complex has entered the atomic age. Structure 17, 1156–1168.

Chi, N.C., Adam, S.A., 1997. Functional domains in nuclear import factor p97 for binding the nuclear localization sequence receptor and the nuclear pore. Mol. Biol. Cell 8, 945–956.

Cronshaw, J.M., Krutchinsky, A.N., Zhang, W., Chait, B.T., Matunis, M.J., 2002. Proteomic analysis of the mammalian nuclear pore complex. J. Cell Biol. 158, 915–927.

Dange, T., Grunwald, D., Grunwald, A., Peters, R., Kubitscheck, U., 2008. Autonomy and robustness of translocation through the nuclear pore complex: a single-molecule study. J. Cell Biol. 183, 77–86.

Denning, D.P., Patel, S.S., Uversky, V., Fink, A.L., Rexach, M., 2003. Disorder in the nuclear pore complex: the FG repeat regions of nucleoporins are natively unfolded. Proc. Natl. Acad. Sci. U. S. A. 100, 2450–2455.

Devos, D., Dokudovskaya, S., Williams, R., Alber, F., Eswar, N., Chait, B.T., Rout, M.P., Sali, A., 2006. Simple fold composition and modular architecture of the nuclear pore complex. Proc. Natl. Acad. Sci. U. S. A. 103, 2172–2177.

Donnert, G., Keller, J., Medda, R., Andrei, M.A., Rizzoli, S.O., Luhrmann, R., Jahn, R., Eggeling, C., Hell, S.W., 2006. Macromolecular-scale resolution in biological fluorescence microscopy. Proc. Natl. Acad. Sci. U. S. A. 103, 11440–11445.

Doye, V., Hurt, E.C., 1995. Genetic approaches to nuclear pore structure and function. Trends Genet. 11, 235–241.

Fahrenkrog, B., Aebi, U., 2003. The nuclear pore complex: nucleocytoplasmic transport and beyond. Nat. Rev. Mol. Cell Biol. 4, 757–766.

Farr, J.C., 2009. Structural and functional analysis of the nuclear pore complex in *Saccharomyces cerevisiae*. PhD thesis, University Münster.

Fink, A.L., 2005. Natively unfolded proteins. Curr. Opin. Struct. Biol. 15, 35–41.

Frey, S., Gorlich, D., 2007. A saturated FG-repeat hydrogel can reproduce the permeability properties of nuclear pore complexes. Cell 130, 512–523.

Frey, S., Richter, R.P., Gorlich, D., 2006. FG-rich repeats of nuclear pore proteins form a three-dimensional meshwork with hydrogel-like properties. Science 314, 815–817.

Grunwald, D., Singer, R.H., 2010. In vivo imaging of labelled endogenous beta-actin mRNA during nucleocytoplasmic transport. Nature 467, 604–607.

Gustafsson, M.G., 2005. Nonlinear structured-illumination microscopy: wide-field fluorescence imaging with theoretically unlimited resolution. Proc. Natl. Acad. Sci. U. S. A. 102, 13081–13086.

Hein, B., Willig, K.I., Hell, S.W., 2008. Stimulated emission depletion (STED) nanoscopy of a fluorescent protein-labeled organelle inside a living cell. Proc. Natl. Acad. Sci. U. S. A. 105, 14271–14276.

Hell, S.W., Stelzer, E.H.K., 1992. Fundamental improvement of resolution with a 4Pi-confocal fluorescence microscope using 2-photon excitation. Opt. Commun. 93, 277–282.

Hess, S.T., Gould, T.J., Gunewardene, M., Bewersdorf, J., Mason, M.D., 2009. Ultrahigh resolution imaging of biomolecules by fluorescence photoactivation localization microscopy. Methods Mol. Biol. 544, 483–522.

Hoppener, C., Siebrasse, J.P., Peters, R., Kubitscheck, U., Naber, A., 2005. High-resolution near-field optical imaging of single nuclear pore complexes under physiological conditions. Biophys. J. 88, 3681–3688.

Hüve, J., Wesselmann, R., Kahms, M., Peters, R., 2008. 4Pi microscopy of the nuclear pore complex. Biophys. J. 95, 877–885.

Isgro, T.A., Schulten, K., 2005. Binding dynamics of isolated nucleoporin repeat regions to importin-beta. Structure 13, 1869–1879.

Isgro, T.A., Schulten, K., 2007. Association of nuclear pore FG-repeat domains to NTF2 import and export complexes. J. Mol. Biol. 366, 330–345.

Izaurralde, E., Kutay, U., von, K.C., Mattaj, I.W., Gorlich, D., 1997. The asymmetric distribution of the constituents of the Ran system is essential for transport into and out of the nucleus. EMBO J. 16, 6535–6547.

Jovanovic-Talisman, T., Tetenbaum-Novatt, J., McKenney, A.S., Zilman, A., Peters, R., Rout, M.P., Chait, B.T., 2009. Artificial nanopores that mimic the transport selectivity of the nuclear pore complex. Nature 457, 1023–1027.

Kahms, M., Lehrich, P., Huve, J., Sanetra, N., Peters, R., 2009. Binding site distribution of nuclear transport receptors and transport complexes in single nuclear pore complexes. Traffic 10, 1228–1242.

Keminer, O., Peters, R., 1999. Permeability of single nuclear pores. Biophys. J. 77, 217–228.
Kiskin, N.I., Siebrasse, J.P., Peters, R., 2003. Optical microwell assay of membrane transport kinetics. Biophys. J. 85, 2311–2322.
Kubitscheck, U., Wedekind, P., Zeidler, O., Grote, M., Peters, R., 1996. Single nuclear pores visualized by confocal microscopy and image processing. Biophys. J. 70, 2067–2077.
Kubitscheck, U., Grunwald, D., Hoekstra, A., Rohleder, D., Kues, T., Siebrasse, J.P., Peters, R., 2005. Nuclear transport of single molecules: dwell times at the nuclear pore complex. J. Cell Biol. 168, 233–243.
Lee, S.J., Matsuura, Y., Liu, S.M., Stewart, M., 2005. Structural basis for nuclear import complex dissociation by RanGTP. Nature 435, 693–696.
Lim, R.Y., Huang, N.P., Koser, J., Deng, J., Lau, K.H., Schwarz-Herion, K., Fahrenkrog, B., Aebi, U., 2006. Flexible phenylalanine–glycine nucleoporins as entropic barriers to nucleocytoplasmic transport. Proc. Natl. Acad. Sci. U. S. A. 103, 9512–9517.
Lim, R.Y., Fahrenkrog, B., Koser, J., Schwarz-Herion, K., Deng, J., Aebi, U., 2007. Nanomechanical basis of selective gating by the nuclear pore complex. Science 318, 640–643.
Lowe, A.R., Siegel, J.J., Kalab, P., Siu, M., Weis, K., Liphardt, J.T., 2010. Selectivity mechanism of the nuclear pore complex characterized by single cargo tracking. Nature 467, 600–603.
Ma, J., Yang, W., 2010. Three-dimensional distribution of transient interactions in the nuclear pore complex obtained from single-molecule snapshots. Proc. Natl. Acad. Sci. U. S. A. 107, 7305–7310.
Mahajan, R., Delphin, C., Guan, T., Gerace, L., Melchior, F., 1997. A small ubiquitin-related polypeptide involved in targeting RanGAP1 to nuclear pore complex protein RanBP2. Cell 88, 97–107.
Mlodzianoski, M.J., Juette, M.F., Beane, G.L., Bewersdorf, J., 2009. Experimental characterization of 3D localization techniques for particle-tracking and super-resolution microscopy. Opt. Express 17, 8264–8277.
Pante, N., Kann, M., 2002. Nuclear pore complex is able to transport macromolecules with diameters of about 39 nm. Mol. Biol. Cell 13, 425–434.
Paradise, A., Levin, M.K., Korza, G., Carson, J.H., 2007. Significant proportions of nuclear transport proteins with reduced intracellular mobilities resolved by fluorescence correlation spectroscopy. J. Mol. Biol. 365, 50–65.
Pemberton, L.F., Paschal, B.M., 2005. Mechanisms of receptor-mediated nuclear import and nuclear export. Traffic 6, 187–198.
Peters, R., 2005. Translocation through the nuclear pore complex: selectivity and speed by reduction-of-dimensionality. Traffic 6, 421–427.
Peters, R., 2006. Introduction to nucleocytoplasmic transport: molecules and mechanisms. Methods Mol. Biol. 322, 235–258.
Peters, R., 2009. Translocation through the nuclear pore: Kaps pave the way. Bioessays 31, 466–477.
Pyhtila, B., Rexach, M., 2003. A gradient of affinity for the karyopherin Kap95p along the yeast nuclear pore complex. J. Biol. Chem. 278, 42699–42709.
Rabut, G., Doye, V., Ellenberg, J., 2004. Mapping the dynamic organization of the nuclear pore complex inside single living cells. Nat. Cell Biol. 6, 1114–1121.
Ribbeck, K., Lipowsky, G., Kent, H.M., Stewart, M., Gorlich, D., 1998. NTF2 mediates nuclear import of Ran. EMBO J. 17, 6587–6598.
Ribbeck, K., Gorlich, D., 2001. Kinetic analysis of translocation through nuclear pore complexes. EMBO J. 20, 1320–1330.
Ribbeck, K., Gorlich, D., 2002. The permeability barrier of nuclear pore complexes appears to operate via hydrophobic exclusion. EMBO J. 21, 2664–2671.
Rout, M.P., Aitchison, J.D., Suprapto, A., Hjertaas, K., Zhao, Y., Chait, B.T., 2000. The yeast nuclear pore complex: composition, architecture, and transport mechanism. J. Cell Biol. 148, 635–651.
Rout, M.P., Aitchison, J.D., Magnasco, M.O., Chait, B.T., 2003. Virtual gating and nuclear transport: the hole picture. Trends Cell Biol. 13, 622–628.
Schermelleh, L., Carlton, P.M., Haase, S., Shao, L., Winoto, L., Kner, P., Burke, B., Cardoso, M.C., Agard, D.A., Gustafsson, M.G., Leonhardt, H., Sedat, J.W., 2008. Subdiffraction multicolor imaging of the nuclear periphery with 3D structured illumination microscopy. Science 320, 1332–1336.
Schmidt, R., Wurm, C.A., Jakobs, S., Engelhardt, J., Egner, A., Hell, S.W., 2008. Spherical nanosized focal spot unravels the interior of cells. Nat. Methods 5, 539–544.
Siebrasse, J.P., Peters, R., 2002. Rapid translocation of NTF2 through the nuclear pore of isolated nuclei and nuclear envelopes. EMBO Rep. 3, 887–892.
Stoffler, D., Fahrenkrog, B., Aebi, U., 1999. The nuclear pore complex: from molecular architecture to functional dynamics. Curr. Opin. Cell Biol. 11, 391–401.
Strambio-De-Castillia, C., Niepel, M., Rout, M.P., 2010. The nuclear pore complex: bridging nuclear transport and gene regulation. Nat. Rev. Mol. Cell Biol. 11, 490–501.
Thompson, R.E., Larson, D.R., Webb, W.W., 2002. Precise nanometer localization analysis for individual fluorescent probes. Biophys. J. 82, 2775–2783.
Timney, B.L., Tetenbaum-Novatt, J., Agate, D.S., Williams, R., Zhang, W., Chait, B.T., Rout, M.P., 2006. Simple kinetic relationships and nonspecific competition govern nuclear import rates in vivo. J. Cell Biol. 175, 579–593.
Tokunaga, M., Imamoto, N., Sakata-Sogawa, K., 2008. Highly inclined thin illumination enables clear single-molecule imaging in cells. Nat. Methods 5, 159–161.
Wente, S.R., Rout, M.P., 2010. The nuclear pore complex and nuclear transport. Cold Spring Harb. Perspect. Biol. 2, a000562.
Wozniak, R., Burke, B., Doye, V., 2010. Nuclear transport and the mitotic apparatus: an evolving relationship. Cell. Mol. Life Sci. 67, 2215–2230.
Yamada, J., Phillips, J.L., Patel, S., Goldfien, G., Calestagne-Morelli, A., Huang, H., Reza, R., Acheson, J., Krishnan, V.V., Newsam, S., Gopinathan, A., Lau, E.Y., Colvin, M.E., Uversky, V.N., Rexach, M.F., 2010. A bimodal distribution of two distinct categories of intrinsically disordered structures with separate functions in FG nucleoporins. Mol. Cell. Proteomics 9, 2205–2224.
Yang, W., Gelles, J., Musser, S.M., 2004. Imaging of single-molecule translocation through nuclear pore complexes. Proc. Natl. Acad. Sci. U. S. A. 101, 12887–12892.
Yildiz, A., Forkey, J.N., McKinney, S.A., Ha, T., Goldman, Y.E., Selvin, P.R., 2003. Myosin V walks hand-over-hand: single fluorophore imaging with 1.5-nm localization. Science 300, 2061–2065.